



Polymer
Chemistry

Organocatalysis in Ring Opening Copolymerization as a Means of Tailoring Molecular Weight Dispersity and the Subsequent Impact on Physical Properties in 4D Printable Photopolymers

Journal:	<i>Polymer Chemistry</i>
Manuscript ID	PY-ART-05-2023-000608.R1
Article Type:	Paper
Date Submitted by the Author:	29-Jun-2023
Complete List of Authors:	Merckle, David; Ohio University, Translational Biosciences Program Weems, Andrew; Ohio University, Mechanical Engineering;

SCHOLARONE™
Manuscripts

Organocatalysis in Ring Opening Copolymerization as a Means of Tailoring Molecular Weight Dispersity and the Subsequent Impact on Physical Properties in 4D Printable Photopolymers

David Merckle¹, Andrew Christopher Weems^{1-2*}

1. Translational Biomedical Sciences, Ohio University, Athens, OH 45701
2. Department of Mechanical Engineering; Biomedical Engineering; Molecular and Chemical Biology; Ohio Musculoskeletal and Neurological Institute, Ohio University, Athens, OH 45701

* corresponding author email: weemsac@ohio.edu

Abstract: Vat photopolymerization 3D printing has traditionally relied on free radical crosslinking between alkenes to produce non-degradable parts, which may have limited use in the biomedical and clinical spaces. Photopolymer resins containing functionalized degradable polymers, specifically polyesters, are greatly interesting for 3D printing tissue scaffolds and medical devices. Unfortunately, most polyesters produced for these applications have been made using metal-containing catalysts, which are not without risk for medical applications. Organocatalysis is a viable alternative route to achieving the same types of polyesters. Here, ring opening copolymerization (ROCOP) of allyl and cyclohexene-containing polyesters is examined using bipyridine and a guanidine-containing catalyst. The role of the catalysts, initiators, and cocatalysts are examined for bulk, open air ROCOP reactions. Unlike previous efforts with organocatalysis, the examined catalysts here could be used to tailor the dispersity of the polyesters, with ~10 kDa polyesters with dispersity ranging from 1.3 to 2.5 examined for the impact on rheological and thermomechanical properties related to resin/part behavior. The bipyridine catalysts and a thiourea cocatalyst further are shown, through the introduction of new fluorescence emissions of the purified polyesters. This work demonstrates that tuning the dispersity of polyester photopolymers provides a direct method of tailoring physical and optical properties in 3D/4D printable materials.

Keywords: Organocatalysis, ring opening copolymerization (ROCOP), 3D/4D printing, polyester, thiol-ene photocrosslinking

Introduction

Additive manufacturing has become one of the most prominent new methods of producing unique or personalized prototypes and devices.¹⁻⁴ 3D printing technology, properly utilized, would provide avenues towards patient-specific implants which are rapidly available in clinical settings. Achieving such a goal requires the parallel development of both the materials platform (the printable materials) as well as the processing methodologies. The hardware component of this, specifically the 3D printing modality which includes considerations such as part stability and resolution, is very advanced and could be competitive with other contemporary medical device or tissue scaffold manufacturing methods.⁵⁻¹¹ The limitation lies with the polymeric materials, and their compatibility/suitability for a given modality, and it is this lack of materials that must be addressed to successfully see patient-specific medical devices enter the clinic at a large scale.

Vat photopolymerization offers a unique balance of mechanical stability, economic flexibility, and throughput that is crucial for personalized medicine.¹⁰ The covalent crosslinking between print layers results in a more mechanically robust part compared with fused filament fabrication, and the use of visible

light lends itself theoretically to a scalable system without increasing user risk.¹⁰ While free-radical crosslinking and epoxide opening are still the most common crosslinking chemistries for vat photopolymerization 3D printing, such materials are often associated with broader property distributions or less reliable tunability, such as with mechanical behaviors or hydrolytic degradation rates.¹²⁻¹⁸ Thiol-ene crosslinking is an alternative gelation mechanism in vat photopolymerizations and 3D printing which provides greater reproducibility and lower variation in properties.^{14, 19-30}

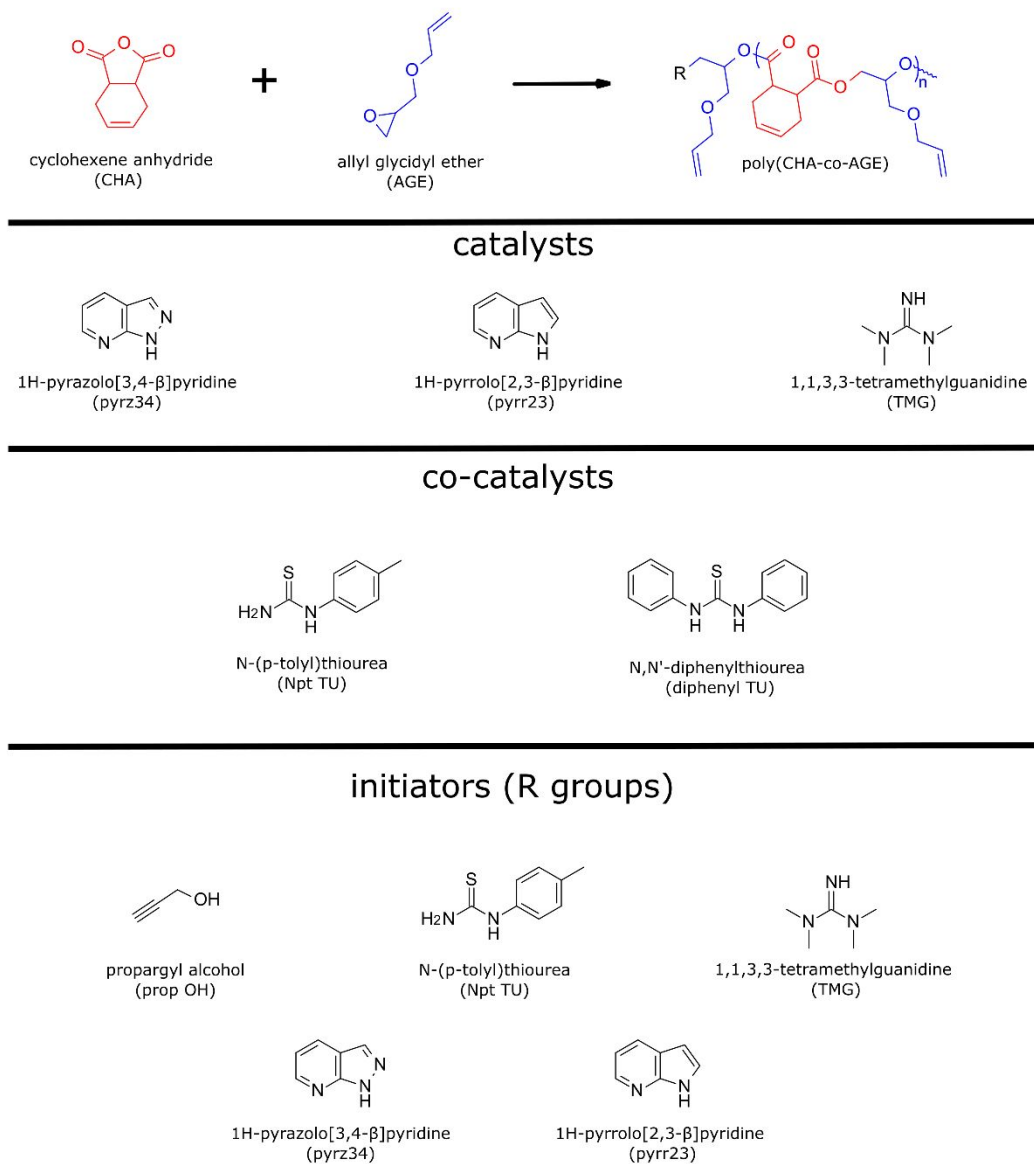
Ring-opening copolymerization (ROCOP) of polyesters provides an opportunity to access photopolymers possessing the necessary functional groups, such as alkenes, necessary for thiol-ene photocrosslinking. The Coates, Darenbourg and Williams groups have been extremely successful, and prolific, with ROCOP for producing stereo-controlled, block, and functional polyesters, but the focus in these works has been on metallic catalysts which are potentially risks for medical applications.^{29, 31-48} The Becker group has similarly explored a magnesium-containing catalyst for the production of poly(propylene fumarate), a polyester which may undergo free radical crosslinking and has found use in vat 3D printing of a variety of tissue scaffolds and medical devices.^{12-16, 49, 50} Using a tin-containing catalyst, Brooks *et al* demonstrated how stereochemistry (both malate and fumarate-containing polyester isomers) as well as stoichiometry (thiol to alkene ratio) could tailor physical properties for photocrosslinkable polyesters.²⁵ While these studies demonstrate the utility of the polyesters for 3D printing, for certain biomedical applications tin and other metal catalysts are a source of concern due to the potential carcinogenic, reproductive toxicity, teratogenicity and developmental problems, and similar risks.⁵¹⁻⁵³ While the metal-based catalysts are very successfully leveraged for ROCOP, exploring organocatalysts which present lower risk profiles could offer significant advantages for the biomedical field.

Organocatalysis is known to provide a number of avenues towards producing polyesters, including the traditional polycondensations as well as by ROCOP mechanisms and other important classes of polymers.^{54, 55} Organic Lewis acid/base pairs have been recently explored as viable routes to making a wide array of polyesters as well as other polymers, as these catalysts may be stereo- or chemoselective as well as resulting in high molecular weights.⁵⁶⁻⁵⁹ Work by Dove and Waymouth demonstrated thiourea/DBU cocatalysts as a means of generating high molecular weight, THF-insoluble poly(lactic acid) with narrow dispersity below 1.2.^{60, 61} The Li group has successfully demonstrated the synthesis of triazine phosphazenes as catalysts for highly selective ROCOP of phthalic anhydride with common epoxides to achieve molecular weights up to ~40 kDa with dispersity below 1.2.⁶² Recently, Merckle *et al* demonstrated the use of functional thioureas co-catalysts with DBU to achieve up to nearly 50 kDa polyesters ($\bar{M}_w < 1.3$) *via* ROCOP in open-air, bulk conditions, demonstrating a simple system with translational potential for various disciplines and industries due to the low barrier for implementation.⁶³ Importantly, the amine-functional thiourea co-catalyst incorporated into the polyester backbone, serving as an initiator for the ROCOP.¹

Control of dispersity has become a growing interest in multiple fields, and with many of the representative organocatalyst studies focusing on narrow molecular weight distributions and high molecular weights, there is an obvious gap in photopolymer material characterization that should be addressed: the role of dispersity in polyester photopolymer physical properties.⁶⁴⁻⁶⁶ As DBU has been shown by numerous authors to be successful for organocatalysis of polyesters and other degradable materials, similar amidine catalysts were considered as viable alternatives.^{20, 26, 60, 61, 63, 67-71} 1,1,3,3-tetramethylguanidine (TMG) has been reported as a commercial and economical alternative to DBU.⁷² As pyrazoles have found use as ligands in ROP of lactide, and due to structural and pKa similarities with DBU, (1H-pyrazolo[3,4- β]pyridine)

and (1H-pyrrolo[2,3- β]pyridine) bipyridinal bases were selected for exploration in the ROCOP of allyl glycidyl ether (AGE) and *cis*-cyclohexene-1,2-dicarboxylic anhydride (CHA), to provide further insight into the role of organocatalysis in this polyester system. We demonstrate the use of these catalysts for tailoring the dispersity of the polyesters while still achieving high molecular weights above 25 kDa. These dispersity differences are then explored for utility in 3D printing photopolymers, comparing viscoelastic and thermomechanical properties while ultimately being used for printing complex prototypes using thiol-ene photocrosslinking.

Results and Discussion



Scheme 1. The idealized structure of the examined monomers and the resultant polyester repeat unit, along with the examined organobase catalysts, thio-urea co-catalysts, and initiators.

The pyrazole 1H-pyrazolo[3,4- β]pyridine (Pyrz34) and pyrrolo species 1H-pyrrolo[2,3- β]pyridine (Pyrr23) were explored as organocatalysts, with two different thioureas (N-(p-tolyl)thiourea (Npt TU) and N,N'-diphenylthiourea (diphenyl TU)) as co-catalysts. Propargyl alcohol, Npt TU, TMG, Pyrz34, and Pyrr23 were examined as initiators as well (Scheme 1). The role of time, catalyst and co-catalyst species, and initiator species was examined for tailoring the molecular weight and dispersity of polyester photopolymers synthesized from AGE and CHA.

The Pyrz34 catalyst, without a co-catalyst or initiator species included, resulted in molecular weights exceeding 20 kDa while maintaining a dispersity below 1.3 for reactions conducted at 100 °C over 48 h. This system further had the benefit of displaying a nearly linear relationship between conversion and molecular weight without dramatically altering the dispersity at any conversion point up to ~90% (Figure 1), and importantly, the resultant polymer displayed ~98% or greater ester linkages over the course of the polymerization, with the final polyester displaying 99% or greater ester linkages (Table 1). The inclusion of the Npt TU and diphenyl TU cocatalyst, or the use of the propargyl alcohol initiator, resulted in similar molecular weights but with dispersity values above 2.0 in all cases. Importantly, the conversion was increased to above 95% with the thioureas and the alcohol initiator. The selectivity of the systems was also not significantly reduced, with more than 98% ester linkages in the final polyester photopolymers.

The Pyrr23 catalyst resulted in 8-10 kDa molecular weights with $1.8 < \bar{D} < 2.6$, where molecular weight growth was linear (relative to conversion) until 90%. Using Npt TU as a co-catalyst resulted in polyesters with molecular weights of approximately 13 kDa, and a dispersity of ~1.6. The highest molecular weight, nearly 29 kDa with a dispersity of up to ~2.4, was achieved when using the diphenyl TU cocatalyst. The incorporation of thioureas Npt TU and diphenyl TU, as well as propargyl alcohol, all resulted in lower molecular weights compared with the Pyrr23 by itself until monomer conversions above 80%.

The TMG catalyst system, regardless of cocatalyst or initiator species examined, resulted in significantly smaller molecular weights (below 5 kDa) with dispersity approaching 2.0. Conversions, unlike with the bicyclic catalysts, ranged from 20% up to 88%, but most TMG catalyst combinations investigated remained between 50 and 70%.

Table 1. Synthetic conditions and characterizations of *cis*-4-cyclohexene-1,2-dicarboxylic anhydride (CHA) and allyl glycidyl ether (AGE) derived polyesters as functions of selected catalyst/co-catalyst and initiator (propargyl alcohol (prop-OH)) combinations. All polymerizations were conducted in bulk, open air, at 100 °C, with a CHA:AGE:catalyst ratio of 200:200:1. (n = 3)

Catalyst/cocatalyst	Time (h)	M _n (NMR) (kDa)	M _n (SEC) (kDa)	TOF (h ⁻¹)	Conversion %	Ester linkage %	Dispersity (\bar{D}) (M _w /M _n)
TMG	1	0.7	0.3	48.4	24.2	84	1.16
	3	0.7	0.3	20.1	60.2	99	1.16
	6	0.8	0.3	11.0	65.8	99	1.16
	12	0.8	0.3	6.3	75.8	90	1.17
	24	1.1	0.3	3.3	78.8	96	1.17
	48	2.4	1.9	1.8	87.6	95	1.70
Pyrr23	1	3.5	5.6	102.8	51.4	99	1.80
	3	12.0	13.1	61.3	91.9	99	2.12
	6	11.7	10.3	31.3	93.8	95	1.94

	12	12.9	12.1	15.7	94.4	97	2.54
	24	9.4	8.8	7.9	94.2	98	1.80
	48	9.3	9.5	4.0	94.8	98	1.88
Pyrz34	1	1.3	2.0	25.0	12.5	98	1.32
	3	3.1	3.1	15.2	22.8	95	1.31
	6	6.1	7.1	16.4	50.2	95	1.33
	12	11.7	12.0	13.0	78.0	95	1.33
	24	13.04	17.7	7.4	89.7	99	1.34
	48	17.8	19.3	3.8	90.0	99	1.34

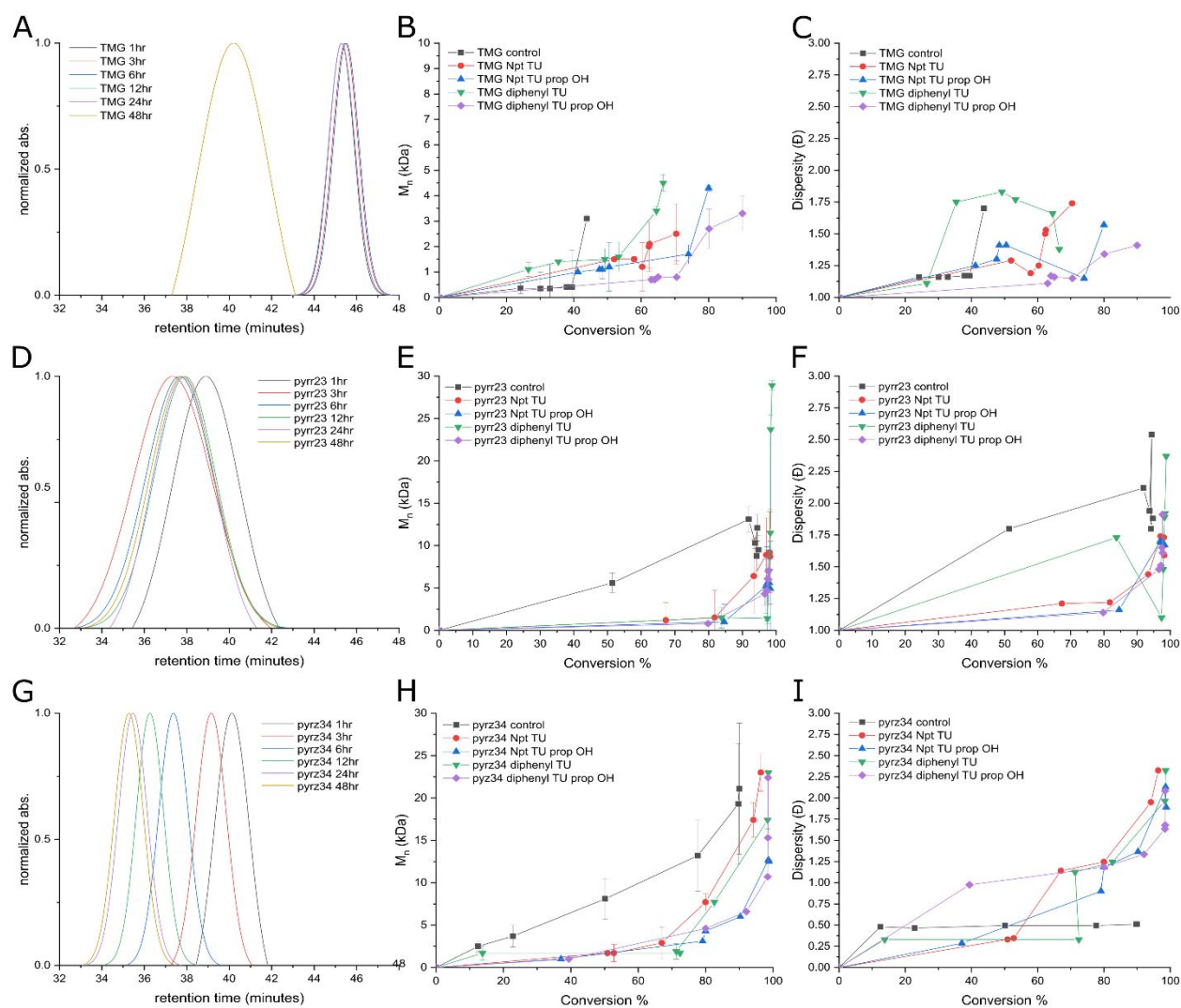


Figure 1. Representative size exclusion chromatography (SEC) curves for ROCOP catalyzed by TMG (A), Pyr23 (D), and Pyr34 (G) as a function of time. Molecular weight and dispersity as functions of conversion for TMG catalyst systems (B, C), Pyr23 catalyst system (E, F) and Pyr34 catalyst systems (H, I). All

polymerizations were conducted in bulk, open air, at 100 °C, with a CHA:AGE:catalyst ratio of 200:200:1 .
(n = 3)

The time required to achieve polyester photopolymers was further examined. Generally, TMG catalyst systems achieved 20 to 60% monomer conversion within the first hour at 100 °C, followed by slow, linear increases over 48 hours up to 80% (Figure 2). This equated to ~15 repeat units maximum achievable with the TMG catalysts. By comparison, the Pyrr23 species displayed 50 to 85% conversion within the first hour, greater than 90% conversion by 2 hours, and 95% conversion by 6 hours for most of the examined catalyst combinations. While the polymerizations were carried out to 48 hours for consistency across the study, there are significantly decreasing returns for prolonging this polymerization as between 50 and 100 repeat units could be achieved within 2-6 hours in a primarily linear relationship (conversion vs molecular weight). By contrast, the Pyr34 catalyst yielded approximately 10 to 50% conversion within the first hour, and up to approximately 85% by 24 hours for all catalyst compositions. This indicates that after 24 h, the same diminishing returns are found for the polymerization with Pyr34. As could be expected, it is at this point that the dispersity begins to significantly increase above 2.0 in most Pyr34 systems. Critically evaluating the results seems to indicate the following behaviors: the Pyrr23 system likely provides the most rapid conversion in comparison with the other two species, regardless of co-catalyst or initiating species. However, the Pyrr23 may also result in the broadest dispersity as well.

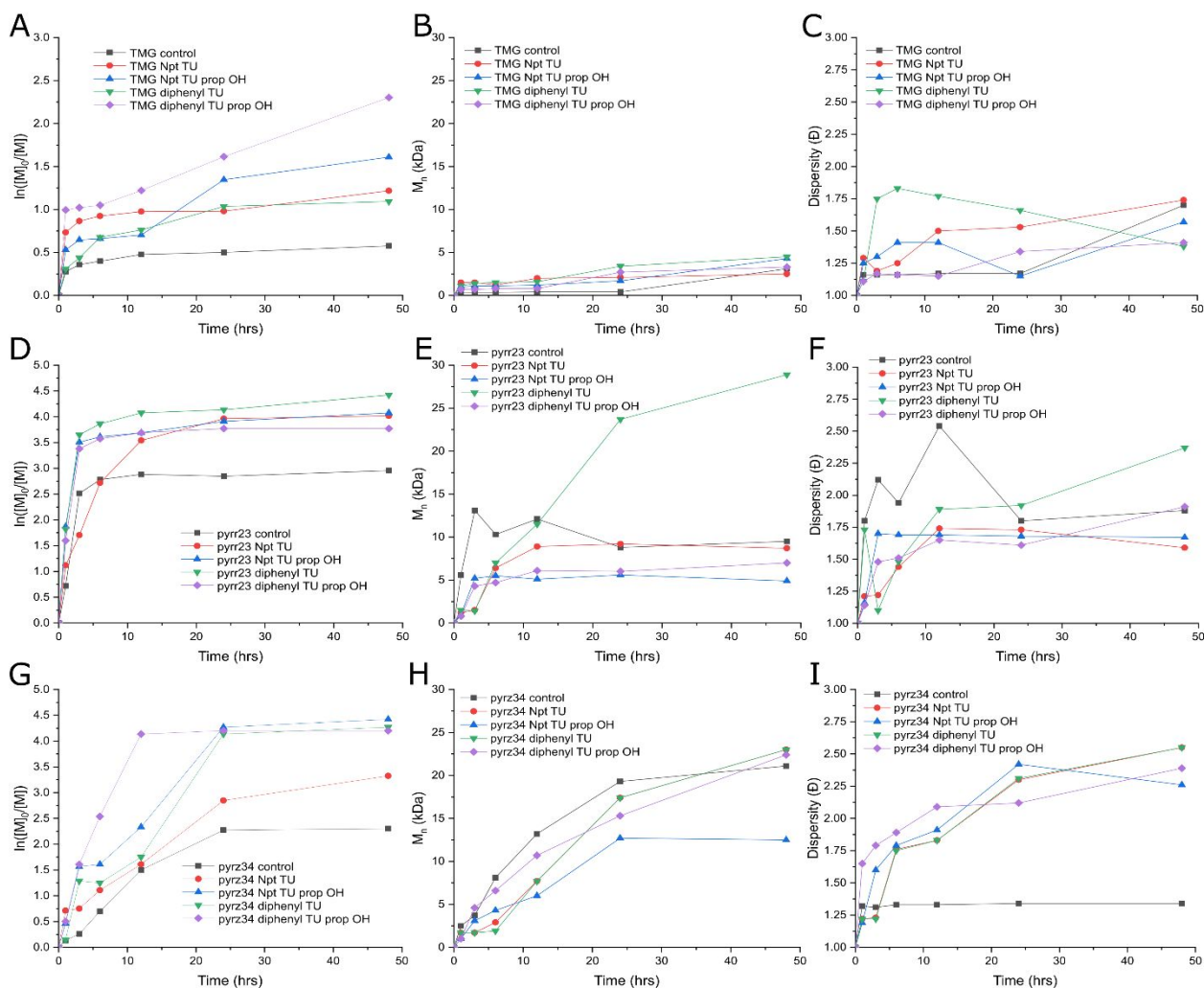


Figure 2. Monomer consumption, molecular weight, and dispersity as functions of time for TMG catalyst systems (A- C), Pyrr23 catalyst system (D-F) and Pyr34 catalyst systems (G-I). All polymerizations were conducted in bulk, open air, at 100 °C, with a CHA:AGE:catalyst ratio of 200:200:1 . (n = 3)

Part of the success of the Pyrr23 and Pyr34 relative to the TMG is likely a similar result to the recent insight by Merckle *et al.*, where Npt TU was shown to incorporate into the polyester backbone during synthesis as indicated by NMR.²² Here, this behavior was found through the fluorescent behavior of the resultant polyesters, which previously did not display such optical properties, indicating the incorporation of certain catalysts that act as initiating species as well (Figure 3).

When polymerized using DBU and propargyl alcohol, the polyesters were found to have an excitation peak at approximately 470 nm but displayed negligible fluorescence emissions (Figure 3B). By comparison, polyesters initiated by the Pyr34 catalyst display an excitation peak centered at ~350 nm and an emission peak at ~430 nm with a tail extending past 650 nm and a full width half maximum (FWHM) of 114 nm. Comparatively, the Pyrr23 initiated polyester displayed an excitation peak at ~420 nm and an emission peak at ~460 nm with a FWHM 91 nm, with a distinctly different emissions curve shape compared to the Pyr34. Importantly, polyesters synthesized as reported by Merckle *et al* using DBU and Npt TU also display fluorescence, where the excitation peak is found at ~340 nm and the emission peak at ~450 nm

with FWHM of 81 nm. These behaviors further indicate that the incorporation reported by Merckle *et al* is found with these bicyclic catalysts as well.²²

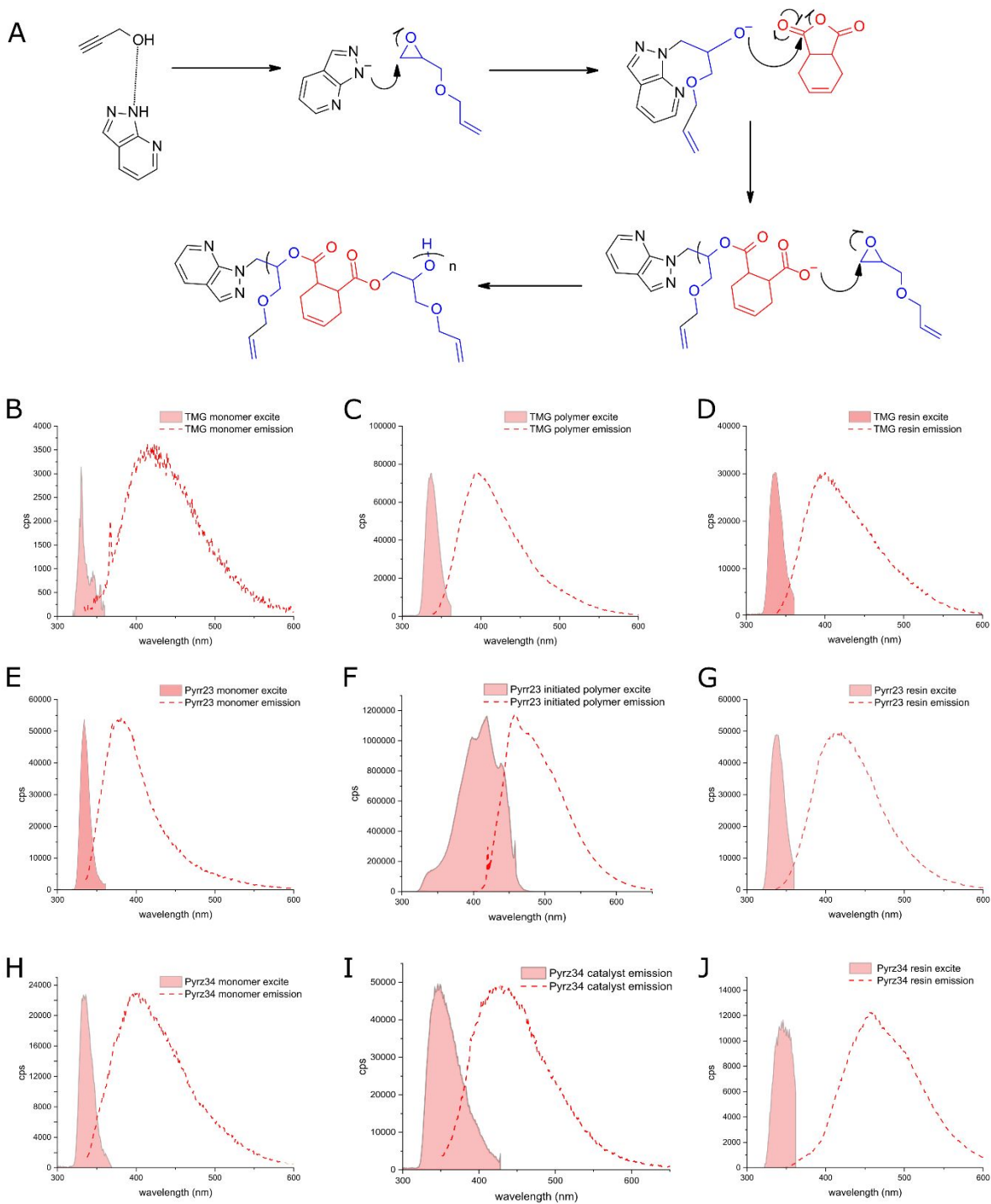


Figure 3. (A) Proposed incorporation mechanism for functional catalyst initiation and incorporation into the polyester backbone and corresponding fluorescence excitation and emission spectra of the resultant polyesters. (B-J) The resulting fluorescence demonstrating the incorporation of the TMG, Pyrr23, and Pyrz34 catalysts into the backbone of the CHA-co-AGE polyester.

As previously noted, using the bicyclic pyridine-type catalysts provided a means with which to produce polyester photopolymers with control over molecular weight dispersity while maintaining the molecular weight and ester linkage content. While Merckle *et al.* indicated that the thermosets produced *via* thiol-ene photocrosslinking (crosslinked using the 4-arm thiol PETMP) do not have a molecular weight dependency at 10 kDa with regards to the elastic moduli and other mechanical properties, it was unclear what the relationship would be with molecular weight dispersity. To that end, polyester photopolymers with molecular weights (M_n) of ~ 10 kDa, with discrete dispersity (\mathcal{D}) distributions of 1.2, 1.5, 2.0, and 2.5 were produced for physical characterization.

Polymer rheological behavior, a critical consideration for vat photopolymerization 3D printing, was examined using unirotational and oscillatory parallel plate shearing. As should be expected for consistent molecular weight, Newtonian fluid polymers with varying dispersity, the dynamic viscosity (μ) was found to increase as the dispersity narrowed (decreased from 2.5 to 1.2) (Figure 4, Table 2). Noticeably, the 1.2 \mathcal{D} species displayed $\mu \sim 593.2 \pm 28.3$ Pa \times s, while 2.5 \mathcal{D} $\mu \sim 22.3 \pm 3.9$ Pa \times s, lower by more than an order of magnitude. For polyester photopolymer resins intended for 3D printing and vat photopolymerizations, this is a critical decrease as the upper threshold for most commercial resins is below 10 Pa \times s.^{26, 73} To achieve this, diluents often utilized for highly viscous polymers, diluent concentrations of up to 50% or more may be required. As the higher dispersity polyesters display viscosity values within the same magnitude as the commercial resins, it is expected that only low concentrations, if any, will be required once the resin is compounded with the thiol crosslinker. For the 2.5 \mathcal{D} photopolymer, compounding a photopolymer resin with an appropriate viscosity, where PETMP has a viscosity of approximately 0.5 Pa \times s, would be readily achievable through a simple stoichiometric balance of thiol to alkene groups, while the 1.2 \mathcal{D} formulation required propylene carbonate or similar diluents.^{22, 74}

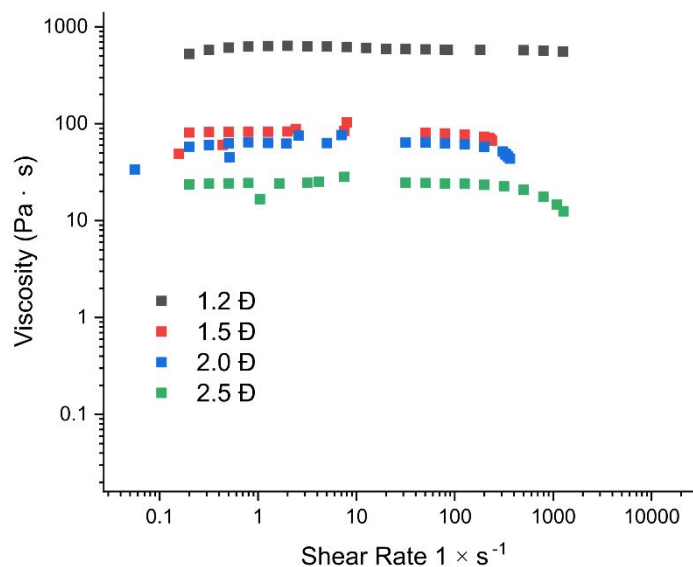


Figure 4. Representative dynamic viscosity as a function of shear rate for ~10 kDa polyesters with different molecular weight distributions, determined from uniaxial parallel plate viscosity. (N = 3, n = 20)

To that end, the photopolymer resin was compounded (stoichiometric balance of in-chain alkenes with PETMP's thiols) (Figure 5A), with Irgacure 819 as the photoinitiator, resulting in a resin that could be crosslinked using visible (405 nm) light. In the 3D printer, these resins could be rapidly processed into porous tissue scaffolds within seconds of irradiation time. Using 0.5 wt% initiator loading, solidification sufficient to stabilize the structure during the peeling and lifting steps was found within 5 s of irradiation at 405 nm. The porous scaffolds were analyzed by microCT (Figure 5B), and were found to be identical, as expected, to previous examples produced using narrow dispersity polyesters reported by Merckle and Brooks, polycarbonates reported by Weems, and bioderived polymyrcene reported by Constant.^{21, 22, 25, 26}

Table 2. Molecular and physical properties of polyester photopolymer and thermosets.

Species: Dispersity (\bar{D}) (M_w/M_n)	M_n (NMR) (kDa)	M_n (SEC) (kDa)	T_g (DSC) (°C)	Viscosity (Pa × s)	E (MPa)	Strain at break (%)	UTS (MPa)	Toughness (MPa × m ²)
1.2 \bar{D}	11.7	11.8	29.2	593.2 ± 28.3	582.7 ± 117.3	10.8 ± 2.2	38.5 ± 8.0	346.2 ± 75.2
1.5 \bar{D}	11.4	11.8	20.8	73.2 ± 19.6	146.7 ± 55.8	23.2 ± 1.4	7.6 ± 1.4	129.8 ± 30.0
2.0 \bar{D}	9.5	8.4	19.8	57.7 ± 10.3	193.9 ± 36.2	33.1 ± 17.8	8.7 ± 1.5	148.3 ± 20.5
2.5 \bar{D}	10.0	9.4	17.5	22.3 ± 3.9	160.0 ± 29.3	7.4 ± 1.9	8.5 ± 0.6	45.0 ± 14.7

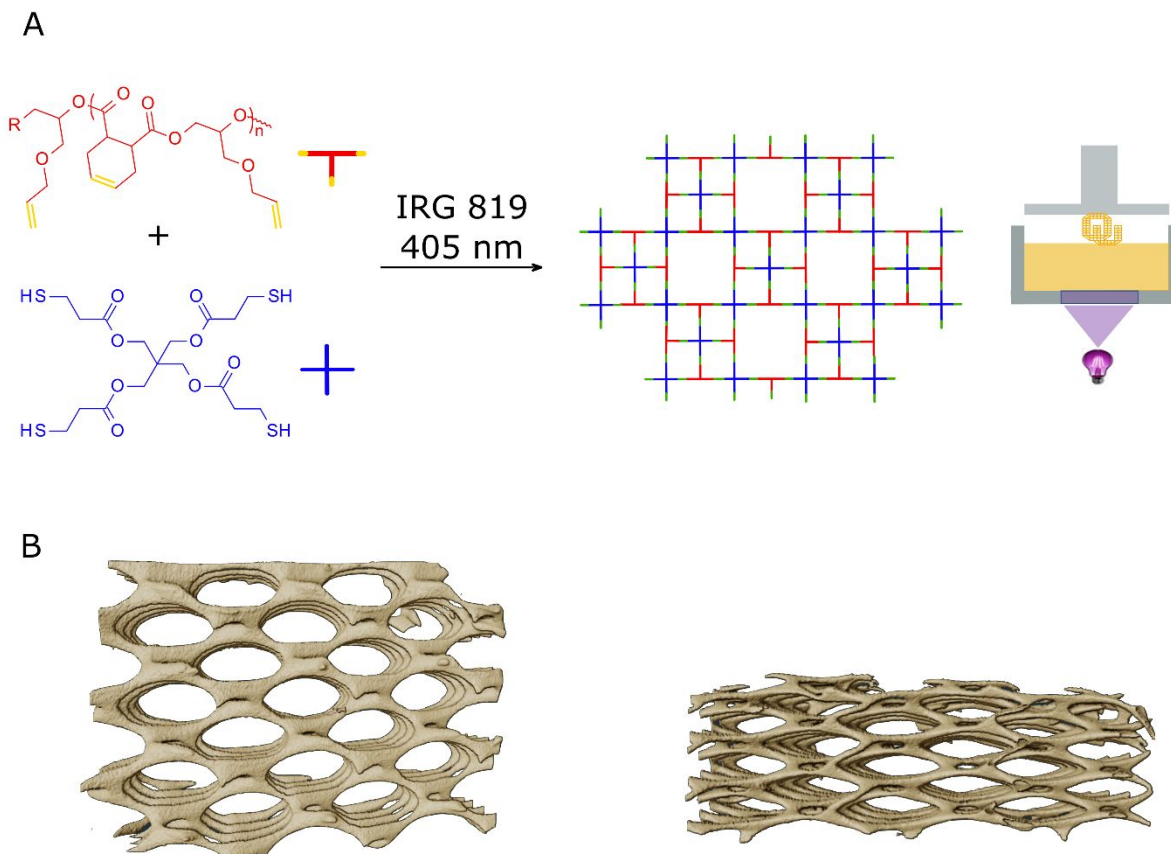


Figure 5. Idealized reaction schematic of pyrazole-initiated poly(AGE-CHA ester) crosslinked with PETMP under 405 nm light to form the thermoset material (A), which was then processed *via* DLP-type 3D printing into a porous scaffold (B) showing the side view (left) and top view (right) that was fixed to the build plate.

The polyester resins were further crosslinked into ASTM Type IV dogbones for monotonic, uniaxial tensile testing for failure analysis, while films were used for thermal analysis by DSC (Figure 6). Thermal analysis supported the rheological performance displayed by the thermoplastic precursors, but in this instance increasing dispersity lowered the glass transition temperature (T_g) of the thermoset. Mechanical property comparisons revealed interesting behaviors for these materials when elongated to failure (Figure 7). For example, the 1.2 \bar{D} samples were statistically more rigid (greater elastic moduli values), while the remaining samples demonstrated no differences between them. Statistically distinct differences were found for other examined properties, as well. Strain at break was found to be statistically lower between the 1.2 \bar{D} and the others, but was greater than the 2.5 \bar{D} .

Interestingly, the 2.5 \bar{D} samples were brittle in a similar manner to the 1.2 \bar{D} species, but to an even greater degree (lower strain at break, statistically). It is hypothesized that this behavior relates to the free volume of the resultant network, where the lower molecular weight diluents serve to increase the network size while simultaneously requiring an increasing number of crosslinks to achieve the “infinite” molecular weight. These two factors likely limit flexibility without influencing the glassy nature of the polyester thermoset network.

The ultimate tensile strength (UTS) also was demonstrated to be dependent upon the dispersity. The lowest examined dispersity, 1.2 \bar{D} , was found to be statistically significant in comparison with the higher dispersity species, the rest of which were not different from each other. For the 1.2 \bar{D} series, the average UTS was approximately 35 MPa while the other values displayed less than 10 MPa UTS. Again, this is likely the result of the plasticizing behavior of the lower molecular weight “impurities” within the networks. Similarly, the toughness of the thermosets followed trend of 1.2 \bar{D} samples being more robust while the higher dispersity samples displayed less durable behavior ($\sim 350 \text{ MPa} \times \text{m}^{-2}$ for 1.2 \bar{D} while the rest of the samples displayed toughness values below $150 \text{ MPa} \times \text{m}^{-2}$). This likely means that cyclic analysis of these samples would also show significant differences with the higher dispersity resulting in more rapid sample degradation under loading. Ultimately, this insight may be used to define the applications for these materials. For example, the narrower dispersity could be targeted towards a specific part, such as a tough and stiff bone tissue scaffold. Alternatively, the broader dispersity samples could find use in general prototyping or as an all-purpose photopolymer resin used to evaluate the structure or stress concentrations as a means of selecting a specific tissue system and design requirements.

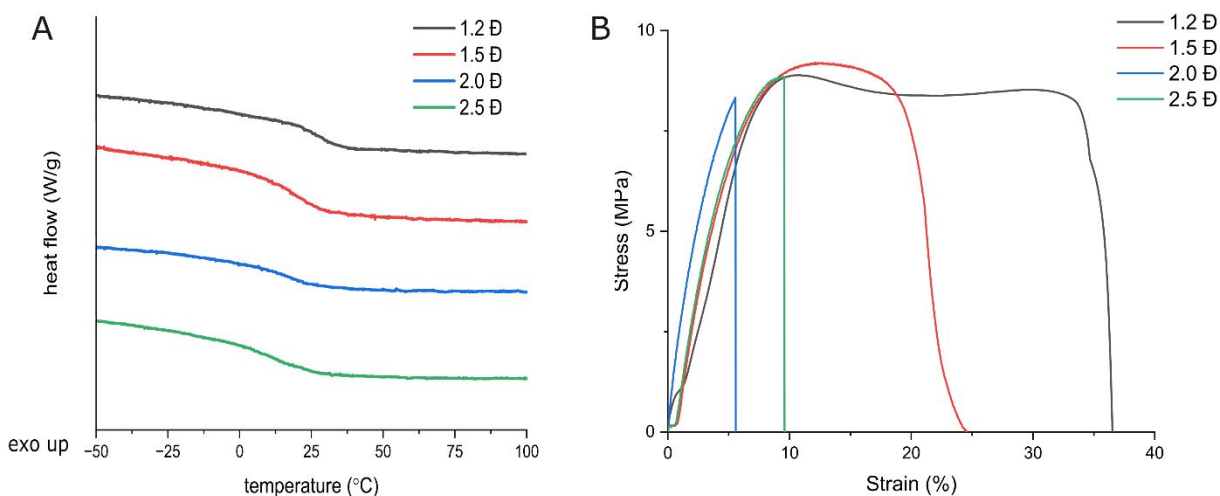


Figure 6. Representative (A) thermograms and (B) tensile stress-strain curves of thermoset polyesters derived from different dispersity photopolymers. (Precursor photopolymer MW ~ 10 kDa by SEC)

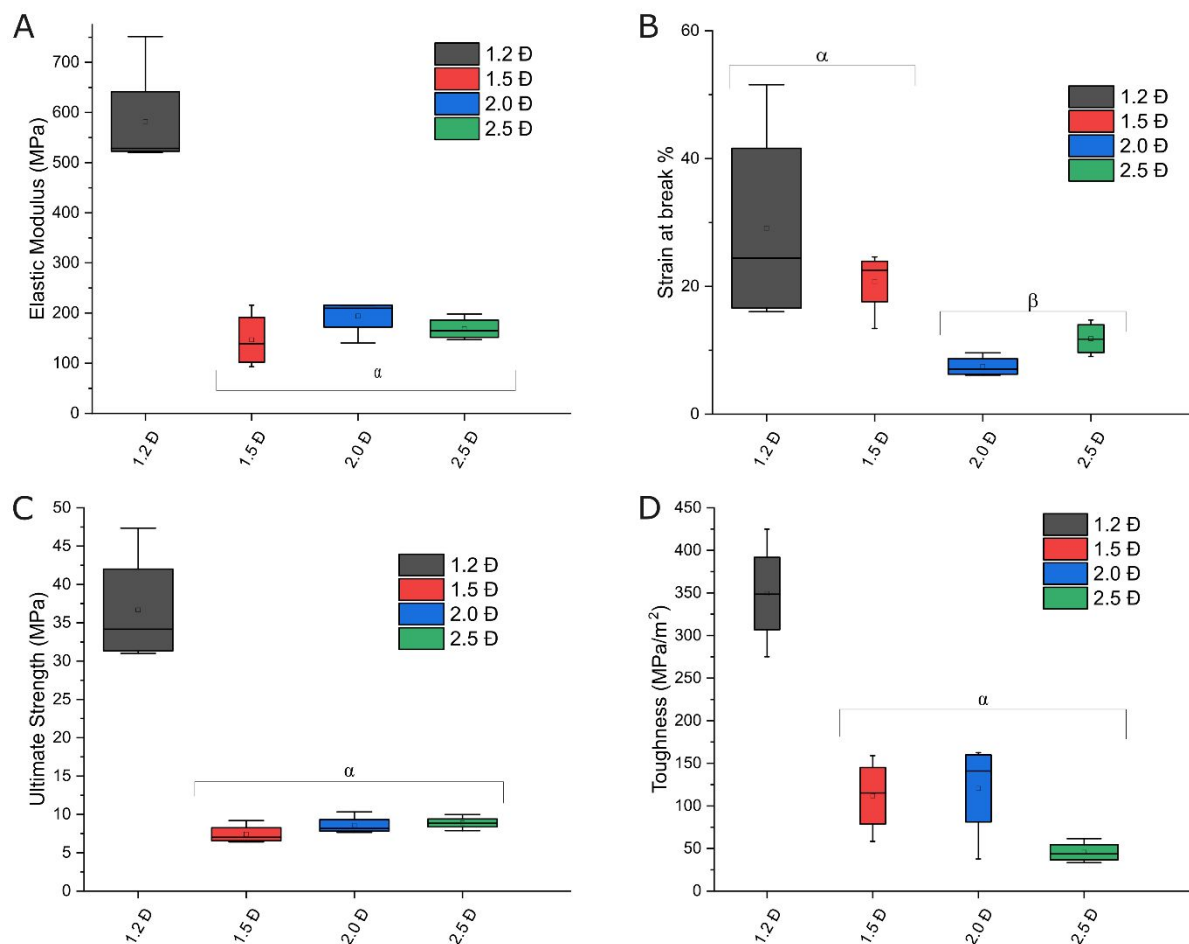


Figure 7. Mechanical properties of dogbones elongated uniaxially to failure, including (A) elastic moduli, (B) strain at break, (C) ultimate tensile strength, and (D) toughness as a function of polyester photopolymer precursor dispersity. (n = 7)

Conclusions

In conclusion, the role of organocatalysts for ROCOP of functional polyesters was explored, providing a route towards tailoring the molecular weight dispersity and influencing the resultant physical properties of crosslinked polyesters. The examined species of bicyclic catalysts provided an opportunity to discretely tailor the dispersity of the resultant polyesters between 1.2 and 2.5 while maintaining a high molecular weight of ~ 25 kDa. Dispersity control was used to examine the thermomechanical behavior of the photopolymers and resultant 3D printed thermosets. Increasing dispersity was found to decrease the viscosity, a benefit for 3D printing resins, but also was shown to decrease the elastic moduli, UTS and toughness of the materials while increasing the strain at break. This tradeoff of physical properties would be useful for exploitation in the design of 3D printable resins with tuned physical behaviors, without altering the molecular weights.

Acknowledgements

The authors would like to acknowledge Ryan Ridgely and Larry Witmer for CT imaging assistance, and the Biomolecular and Chemical Engineering Department for use of the fluorimeter. D Merckle is supported by the DoE (19361-23-1136602).

Supplementary Materials

¹H NMR spectra, SEC traces, rheological behaviors, raw tensile data are available in the Supplementary Materials document here.

Conflicts of Interest

None to report.

References

- (1) Ahangar, P.; Cooke, M. E.; Weber, M. H.; Rosenzweig, D. H. Current Biomedical Applications of 3D Printing and Additive Manufacturing. *Appl. Sci.* **2019**, *9* (8). DOI: 10.3390/app9081713.
- (2) Berretta, S.; Evans, K.; Ghita, O. Additive manufacture of PEEK cranial implants: Manufacturing considerations versus accuracy and mechanical performance. *Mater. Des.* **2018**, *139*, 141-152. DOI: 10.1016/j.matdes.2017.10.078.
- (3) Guggenbiller, G.; Brooks, S.; King, O.; Constant, E.; Merckle, D.; Weems, A. C. 3D Printing of Green and Renewable Polymeric Materials: Toward Greener Additive Manufacturing. *ACS Applied Polymer Materials* **2023**. DOI: 10.1021/acsapm.2c02171.
- (4) Weems, A. C.; Perez-Madrigal, M. M.; Arno, M. C.; Dove, A. P. 3D Printing for the Clinic: Examining Contemporary Polymeric Biomaterials and Their Clinical Utility. *Biomacromolecules* **2020**, *21* (3), 1037-1059. DOI: 10.1021/acs.biomac.9b01539.
- (5) de Beer, M. P. v. d. L., H.L.; Cole, M.A.; Whelan, R.J.; Burns, M.A.; Scott, T.F. Rapid, Continuous Additive Manufacturing by Volumetric Polymerization Inhibition Patterning. *Sci. Adv.* **2019**, *5* (1).
- (6) Kelly, B. E. B., I.; Heidari, H.; Shusteff, M.; Spadaccini, C.M.; Taylor, H.K. Volumetric additive manufacturing via tomographic reconstruction. *Science* **2019**, *363*, 1075-1079.
- (7) Shusteff, M. B., A.M.E.; Kelly, B.E.; Henriksson, J.; Weisgraber, T.H.; Panas, R.M.; Fang, N.X.; Spadaccini, C.M. One-step volumetric additive manufacturing of complex polymer structures. *Sci. Adv.* **2017**, *3*, eaao5496.
- (8) Tumbleston, J. R. S., D.; Ermoshkin, N.; Januszewicz, R.; Johnson, A.R.; Kelly, D.; Chen, K; Pinschmidt, R; Rolland, J.P.; Ermoshkin, A.; Samulski, E.T.; DeSimone, J.M. Continuous Liquid Interface Production of 3D Objects. *Science* **2015**, *347* (6228), 1349-1352.
- (9) Chia, H. N.; Wu, B. M. Recent advances in 3D printing of biomaterials. *J Biol Eng* **2015**, *9*, 4. DOI: 10.1186/s13036-015-0001-4.
- (10) Ligon, S. C.; Liska, R.; Stampfl, J.; Gurr, M.; Mulhaupt, R. Polymers for 3D Printing and Customized Additive Manufacturing. *Chem Rev* **2017**, *117* (15), 10212-10290. DOI: 10.1021/acs.chemrev.7b00074.
- (11) Walker, D. A. H., J.L.; Mirkin, C.A. Rapid, large-volume, thermally controlled 3D printing using a mobile liquid interface. *Science* **2019**, *366*, 360-364.
- (12) Childers, E. P.; Wang, M. O.; Becker, M. L.; Fisher, J. P.; Dean, D. 3D printing of resorbable poly(propylene fumarate) tissue engineering scaffolds. *MRS Bull.* **2015**, *40* (2), 119-126. DOI: 10.1557/mrs.2015.2.
- (13) Dilla, R. A.; Motta, C. M. M.; Snyder, S. R.; Wilson, J. A.; Wesdemiotis, C.; Becker, M. L. Synthesis and 3D Printing of PEG-Poly(propylene fumarate) Diblock and Triblock Copolymer Hydrogels. *ACS Macro. Lett.* **2018**, *7* (10), 1254-1260. DOI: 10.1021/acsmacrolett.8b00720.

- (14) Kirillova, A.; Yeazel, T. R.; Gall, K.; Becker, M. L. Thiol-Based Three-Dimensional Printing of Fully Degradable Poly(propylene fumarate) Star Polymers. *ACS Appl. Mater. Interfaces* **2022**, *14* (34), 38436-38447. DOI: 10.1021/acsami.2c06553 From NLM PubMed-not-MEDLINE.
- (15) Luo, Y.; Dolder, C. K.; Walker, J. M.; Mishra, R.; Dean, D.; Becker, M. L. Synthesis and Biological Evaluation of Well-Defined Poly(propylene fumarate) Oligomers and Their Use in 3D Printed Scaffolds. *Biomacromolecules* **2016**, *17* (2), 690-697. DOI: 10.1021/acs.biomac.6b00014.
- (16) Luo, Y.; Le Fer, G.; Dean, D.; Becker, M. L. 3D Printing of Poly(propylene fumarate) Oligomers: Evaluation of Resin Viscosity, Printing Characteristics and Mechanical Properties. *Biomacromolecules* **2019**, *20* (4), 1699-1708. DOI: 10.1021/acs.biomac.9b00076.
- (17) Petersen, S. R.; Wilson, J. A.; Becker, M. L. Versatile Ring-Opening Copolymerization and Postprinting Functionalization of Lactone and Poly(propylene fumarate) Block Copolymers: Resorbable Building Blocks for Additive Manufacturing. *Macromolecules* **2018**, *51* (16), 6202-6208. DOI: 10.1021/acs.macromol.8b01372.
- (18) Walker, J. M.; Bodamer, E.; Krebs, O.; Luo, Y.; Kleinfehn, A.; Becker, M. L.; Dean, D. Effect of Chemical and Physical Properties on the In Vitro Degradation of 3D Printed High Resolution Poly(propylene fumarate) Scaffolds. *Biomacromolecules* **2017**, *18* (4), 1419-1425. DOI: 10.1021/acs.biomac.7b00146.
- (19) Brooks, S.; Cartwright, Z.; Merckle, D.; Weems, A. C. 4D Aliphatic photopolymer polycarbonates as direct ink writing of biodegradable, conductive graphite-composite materials. *Polym. Compos.* **2021**, 1-10. DOI: 10.1002/pc.26211.
- (20) Brooks, S. L. A., M.C.; Dove, A.P.; Weems, A.C. Postfabrication Functionalization of 4D-Printed Polycarbonate Photopolymer Scaffolds. *ACS Appl Polym Mater* **2022**, ASAP. DOI: 10.1021/acsapm.2c00648.
- (21) Constant, E.; King, O.; Weems, A. C. Bioderived 4D Printable Terpene Photopolymers from Limonene and beta-Myrcene. *Biomacromolecules* **2022**, *23* (6), 2342-2352. DOI: 10.1021/acs.biomac.2c00085 From NLM Medline.
- (22) David Merckle, O. King., Andrew C Weems. Ring-Opening Copolymerization of Four-Dimensional Printable Polyesters Using Supramolecular Thiourea/Organocatalysis. *ACS Sustain. Chem. Eng.* **2023**, *11* (6), 2219-2228. <https://doi.org/10.1021/acssuschemeng.2c05552>.
- (23) Merckle, D.; Constant, E.; Cartwright, Z.; Weems, A. Ring Opening Copolymerization (ROCOP) of 4D Printed Shape Memory Polyester Photopolymers using Digital Light Processing. *Macromolecules* **2021**, *54* (6), 2681-2690.
- (24) Merckle, D.; Constant, E.; Weems, A. C. Linalool Derivatives for Natural Product-Based 4D Printing Resins. *ACS Sustainable Chemistry & Engineering* **2021**, *9* (36), 12213-12222. DOI: 10.1021/acssuschemeng.1c03760.
- (25) SL Brooks, E. C., OM King, AC Weems. Stereochemistry and stoichiometry in aliphatic polyester photopolymers for 3D printing tailored biomaterial scaffolds. *Polym. Chem.* **2022**, *13* (14), 2048-2056.
- (26) Weems, A. C.; Arno, M. C. A.; Huckstepp, R. T. R.; Dove, A. P. 4D Polycarbonates via Stereolithography as Scaffolds for Soft Tissue Repair *Nat. Commun.* **2021**, *12* (1), 1-14.
- (27) Weems, A. C.; Delle Chiaie, K. R.; Yee, R.; Dove, A. P. Selective Reactivity of Myrcene for Vat Photopolymerization 3D Printing and Post-Fabrication Surface Modification. *Biomacromolecules* **2019**, *21* (1), 163-170. DOI: 10.1021/acs.biomac.9b01125.
- (28) Roppolo, I.; Frascella, F.; Gastaldi, M.; Castellino, M.; Ciubini, B.; Barolo, C.; Scaltrito, L.; Nicosia, C.; Zanetti, M.; Chiappone, A. Thiol-yne chemistry for 3D printing: exploiting an off-stoichiometric route for selective functionalization of 3D objects. *Polym. Chem.* **2019**, *10* (44), 5950-5958. DOI: 10.1039/c9py00962k.

- (29) Wei, P.; Bhat, G. A.; Cipriani, C. E.; Mohammad, H.; Schoonover, K.; Pentzer, E. B.; Darensbourg, D. J. 3D Printed CO₂-Based Triblock Copolymers and Post-Printing Modification. *Angew. Chem. Int. Ed.* **2022**, *61* (37), e202208355, <https://doi.org/10.1002/anie.202208355>. DOI: <https://doi.org/10.1002/anie.202208355> (accessed 2022/10/08).
- (30) Weems, A. C. C., K.R.D.; Worch, J.C.; Stubbs, C.J.; Dove, A.P. Terpene-based Polymeric Resins for Stereolithography 3D Printing. *Polym. Chem.* **2019**, *10* (44), 5959-5966.
- (31) Abel, B. A.; Lidston, C. A. L.; Coates, G. W. Mechanism-Inspired Design of Bifunctional Catalysts for the Alternating Ring-Opening Copolymerization of Epoxides and Cyclic Anhydrides. *J. Am. Chem. Soc.* **2019**, *141* (32), 12760-12769. DOI: 10.1021/jacs.9b05570.
- (32) DiCiccio, A. M.; Coates, G. W. Ring-opening copolymerization of maleic anhydride with epoxides: a chain-growth approach to unsaturated polyesters. *J. Am. Chem. Soc.* **2011**, *133* (28), 10724-10727. DOI: 10.1021/ja203520p.
- (33) Longo, J. M.; Sanford, M. J.; Coates, G. W. Ring-Opening Copolymerization of Epoxides and Cyclic Anhydrides with Discrete Metal Complexes: Structure-Property Relationships. *Chem Rev* **2016**, *116* (24), 15167-15197. DOI: 10.1021/acs.chemrev.6b00553.
- (34) Carrodeguas, L. P.; Chen, T. T. D.; Gregory, G. L.; Sulley, G. S.; Williams, C. K. High Elasticity, Chemically Recyclable, Thermoplastics from Bio-Based Monomers: Carbon Dioxide, Limonene Oxide and ϵ -Decalactone. *Green Chemistry* **2020**, *22* (23), 8298-8307. DOI: 10.1039/d0gc02295k.
- (35) Chen, T. T. D.; Carrodeguas, L. P.; Sulley, G. S.; Gregory, G. L.; Williams, C. K. Bio-based and Degradable Block Polyester Pressure-Sensitive Adhesives. *Angew. Chem. Int. Ed. Engl.* **2020**, *59* (52), 23450-23455. DOI: 10.1002/anie.202006807 From NLM Medline.
- (36) Chen, T. T. D.; Zhu, Y.; Williams, C. K. Pentablock Copolymer from Tetracomponent Monomer Mixture Using a Switchable Zinc Catalyst. *Macromolecules* **2018**, *51* (14), 5346-5351. DOI: 10.1021/acs.macromol.8b01224.
- (37) Garden, J. A.; Saini, P. K.; Williams, C. K. Greater than the Sum of Its Parts: A Heterodinuclear Polymerization Catalyst. *J. Am. Chem. Soc.* **2015**, *137* (48), 15078-15081. DOI: 10.1021/jacs.5b09913.
- (38) Gregory, G. L.; Sulley, G. S.; Carrodeguas, L. P.; Chen, T. T. D.; Santmarti, A.; Terrill, N. J.; Lee, K.-Y.; Williams, C. K. Triblock polyester thermoplastic elastomers with semi-aromatic polymer end blocks by ring-opening copolymerization. *Chemical Science* **2020**, *11* (25), 6567-6581. DOI: 10.1039/d0sc00463d.
- (39) Paul, S.; Romain, C.; Shaw, J.; Williams, C. K. Sequence Selective Polymerization Catalysis: A New Route to ABA Block Copoly(ester-b-carbonate-b-ester). *Macromolecules* **2015**, *48* (17), 6047-6056. DOI: 10.1021/acs.macromol.5b01293.
- (40) Paul, S.; Zhu, Y.; Romain, C.; Brooks, R.; Saini, P. K.; Williams, C. K. Ring-opening copolymerization (ROCOP): synthesis and properties of polyesters and polycarbonates. *Chem Commun (Camb)* **2015**, *51* (30), 6459-6479. DOI: 10.1039/c4cc10113h.
- (41) Sulley, G. S.; Gregory, G. L.; Chen, T. T. D.; Pena Carrodeguas, L.; Trott, G.; Santmarti, A.; Lee, K. Y.; Terrill, N. J.; Williams, C. K. Switchable Catalysis Improves the Properties of CO₂-Derived Polymers: Poly(cyclohexene carbonate-b-epsilon-decalactone-b-cyclohexene carbonate) Adhesives, Elastomers, and Toughened Plastics. *J. Am. Chem. Soc.* **2020**, *142* (9), 4367-4378. DOI: 10.1021/jacs.9b13106.
- (42) Thevenon, A.; Garden, J. A.; White, A. J.; Williams, C. K. Dinuclear Zinc Salen Catalysts for the Ring Opening Copolymerization of Epoxides and Carbon Dioxide or Anhydrides. *Inorg. Chem.* **2015**, *54* (24), 11906-11915. DOI: 10.1021/acs.inorgchem.5b02233.
- (43) Yi, N.; Chen, T. T. D.; Unruangsri, J.; Zhu, Y.; Williams, C. K. Orthogonal functionalization of alternating polyesters: selective patterning of (AB)_n sequences. *Chem Sci* **2019**, *10* (43), 9974-9980. DOI: 10.1039/c9sc03756j.
- (44) Zhu, Y.; Radlauer, M. R.; Schneiderman, D. K.; Shaffer, M. S. P.; Hillmyer, M. A.; Williams, C. K. Multiblock Polyesters Demonstrating High Elasticity and Shape Memory Effects. *Macromolecules* **2018**, *51* (7), 2466-2475. DOI: 10.1021/acs.macromol.7b02690.

- (45) Darensbourg, D. J.; Poland, R. R.; Escobedo, C. Kinetic Studies of the Alternating Copolymerization of Cyclic Acid Anhydrides and Epoxides, and the Terpolymerization of Cyclic Acid Anhydrides, Epoxides, and CO₂ Catalyzed by (salen)Cr(III)Cl. *Macromolecules* **2012**, *45* (5), 2242-2248. DOI: 10.1021/ma2026385.
- (46) Darensbourg, D. J.; Wu, G.-P. A One-Pot Synthesis of a Triblock Copolymer from Propylene Oxide/Carbon Dioxide and Lactide: Intermediacy of Polyol Initiators. *Angew. Chem. Int. Ed.* **2013**, *52* (40), 10602-10606, <https://doi.org/10.1002/anie.201304778>. DOI: <https://doi.org/10.1002/anie.201304778> (accessed 2022/10/12).
- (47) Wu, G. P.; Darensbourg, D. J.; Lu, X. B. Tandem metal-coordination copolymerization and organocatalytic ring-opening polymerization via water to synthesize diblock copolymers of styrene oxide/CO₂ and lactide. *J. Am. Chem. Soc.* **2012**, *134* (42), 17739-17745. DOI: 10.1021/ja307976c From NLM Medline.
- (48) Zhang, Y.-Y.; Wu, G.-P.; Darensbourg, D. J. CO₂-Based Block Copolymers: Present and Future Designs. *Trends in Chemistry* **2020**, *2* (8), 750-763. DOI: 10.1016/j.trechm.2020.05.002.
- (49) Kleinfehn, A. P.; Lammel Lindemann, J. A.; Razvi, A.; Philip, P.; Richardson, K.; Nettleton, K.; Becker, M. L.; Dean, D. Modulating Bioglass Concentration in 3D Printed Poly(propylene fumarate) Scaffolds for Post-Printing Functionalization with Bioactive Functional Groups. *Biomacromolecules* **2019**, *20* (12), 4345-4352. DOI: 10.1021/acs.biomac.9b00941.
- (50) Wilson, J. A.; Luong, D.; Kleinfehn, A. P.; Sallam, S.; Wesdemiotis, C.; Becker, M. L. Magnesium Catalyzed Polymerization of End Functionalized Poly(propylene maleate) and Poly(propylene fumarate) for 3D Printing of Bioactive Scaffolds. *J. Am. Chem. Soc.* **2018**, *140* (1), 277-284. DOI: 10.1021/jacs.7b09978.
- (51) Genchi, G.; Carocci, A.; Lauria, G.; Sinicropi, M. S.; Catalano, A. Nickel: Human Health and Environmental Toxicology. *Int J Environ Res Public Health* **2020**, *17* (3). DOI: 10.3390/ijerph17030679 From NLM Medline.
- (52) ADMINISTRATION, U. F. A. D. *Use of International Standard ISO 10993-1, "Biological Evaluation of Medical Devices - Part 1: Evaluation and Testing Within a Risk Management Process"*; FDA, Silver Spring, MD, 2020.
- (53) Harper, C. L., F.; Diamond, G.; Chappell, L.L. TOXICOLOGICAL PROFILE FOR TIN AND TIN COMPOUNDS. In *A Toxicological Profile for Tin and Tin Compounds, Draft for Public Comment*, Service, U. S. D. O. H. A. H. S. P. H., Registry, A. f. T. S. a. D., Eds.; 2005.
- (54) Bossion, A.; Heifferon, K. V.; Meabe, L.; Zivic, N.; Taton, D.; Hedrick, J. L.; Long, T. E.; Sardon, H. Opportunities for organocatalysis in polymer synthesis via step-growth methods. *Progress in Polymer Science* **2019**, *90*, 164-210. DOI: 10.1016/j.progpolymsci.2018.11.003.
- (55) Sardon, H.; Pascual, A.; Mecerreyes, D.; Taton, D.; Cramail, H.; Hedrick, J. L. Synthesis of Polyurethanes Using Organocatalysis: A Perspective. *Macromolecules* **2015**, *48* (10), 3153-3165. DOI: 10.1021/acs.macromol.5b00384.
- (56) Chen, Y.; Shen, J.; Liu, S.; Zhao, J.; Wang, Y.; Zhang, G. High Efficiency Organic Lewis Pair Catalyst for Ring-Opening Polymerization of Epoxides with Chemoselectivity. *Macromolecules* **2018**, *51* (20), 8286-8297. DOI: 10.1021/acs.macromol.8b01852.
- (57) Hu, L.-F.; Zhang, C.-J.; Wu, H.-L.; Yang, J.-L.; Liu, B.; Duan, H.-Y.; Zhang, X.-H. Highly Active Organic Lewis Pairs for the Copolymerization of Epoxides with Cyclic Anhydrides: Metal-Free Access to Well-Defined Aliphatic Polyesters. *Macromolecules* **2018**, *51* (8), 3126-3134. DOI: 10.1021/acs.macromol.8b00499.
- (58) Hu, L. F.; Chen, D. J.; Yang, J. L.; Zhang, X. H. An Investigation of the Organoborane/Lewis Base Pairs on the Copolymerization of Propylene Oxide with Succinic Anhydride. *Molecules* **2020**, *25* (2). DOI: 10.3390/molecules25020253.

- (59) Ji, H.-Y.; Song, D.-P.; Wang, B.; Pan, L.; Li, Y.-S. Organic Lewis pairs for selective copolymerization of epoxides with anhydrides to access sequence-controlled block copolymers. *Green Chemistry* **2019**, *21* (22), 6123-6132. DOI: 10.1039/c9gc02429h.
- (60) Dove, A. P., RC; Lohmeijer, BGG; Waymouth, RM; Hedrick, JL. Thiourea-Based Bifunctional Organocatalysis: Supramolecular Recognition for Living Polymerization. *Journal of the American Chemical Society* **2005**, *127*, 13798-13799.
- (61) Dove, A. P. Organic Catalysis for Ring-Opening Polymerization. *ACS Macro. Lett.* **2012**, *1* (12), 1409-1412. DOI: 10.1021/mz3005956.
- (62) Wang, L.; Zhang, J.; Zhao, N.; Ren, C.; Liu, S.; Li, Z. Synthesis of Tris-Phosphazene Bases with Triazine as Core and Their Applications for Efficient Ring-Opening Alternating Copolymerization of Epoxide and Anhydride: Notable Effect of Basicity and Molecular Size. *ACS Macro Lett* **2020**, *9* (9), 1398-1402. DOI: 10.1021/acsmacrolett.0c00564 From NLM PubMed-not-MEDLINE.
- (63) Merckle, D.; King, O.; Weems, A. C. Ring-Opening Copolymerization of Four-Dimensional Printable Polyesters Using Supramolecular Thiourea/Organocatalysis. *ACS Sustainable Chemistry & Engineering* **2023**, *11* (6), 2219-2228. DOI: 10.1021/acssuschemeng.2c05552.
- (64) Walsh, D. J.; Schinski, D. A.; Schneider, R. A.; Guironnet, D. General route to design polymer molecular weight distributions through flow chemistry. *Nat Commun* **2020**, *11* (1), 3094. DOI: 10.1038/s41467-020-16874-6.
- (65) Whitfield, R.; Truong, N. P.; Messmer, D.; Parkatzidis, K.; Rolland, M.; Anastasaki, A. Tailoring polymer dispersity and shape of molecular weight distributions: methods and applications. *Chem Sci* **2019**, *10* (38), 8724-8734. DOI: 10.1039/c9sc03546j From NLM PubMed-not-MEDLINE.
- (66) Antonopoulou, M.-N.; Whitfield, R.; Truong, N. P.; Wyers, D.; Harrisson, S.; Junkers, T.; Anastasaki, A. Concurrent control over sequence and dispersity in multiblock copolymers. *Nature Chemistry* **2022**, *14* (3), 304-312. DOI: 10.1038/s41557-021-00818-8.
- (67) Arno, M. C.; Brannigan, R. P.; Policastro, G. M.; Becker, M. L.; Dove, A. P. pH-Responsive, Functionalizable Spyrocyclic Polycarbonate: A Versatile Platform for Biocompatible Nanoparticles. *Biomacromolecules* **2018**, *19* (8), 3427-3434. DOI: 10.1021/acs.biomac.8b00744.
- (68) Bas G. G. Lohmeijer, R. C. P., † Frank Leibfarth, ‡ John W. Logan, †, § David A. Long, | Andrew P. Dove, † Fredrik Nederberg, †, # Jeongsoo Choi, † Charles Wade, † Robert M. Waymouth, *, # and James L. Hedrick*, †. Guanidine and Amidine Organocatalysts for Ring-Opening Polymerization of Cyclic Esters. *Macromolecules* **2006**, *39*, 8574-8583.
- (69) Fredrik Nederberg, ‡ Bas G. G. Lohmeijer, †, ‡ Frank Leibfarth, † Russell C. Pratt, † Jeongsoo Choi, † Andrew P. Dove, § Robert M. Waymouth, *, ‡ and James L. Hedrick*, . Organocatalytic Ring Opening Polymerization of Trimethylene Carbonate. *Biomacromolecules* **2007**, *8*, 153-160.
- (70) Lohmeijer, B. G. G.; Pratt, R. C.; Leibfarth, F.; Logan, J. W.; Long, D. A.; Dove, A. P.; Nederberg, F.; Choi, J.; Wade, C.; Waymouth, R. M.; et al. Guanidine and Amidine Organocatalysts for Ring-Opening Polymerization of Cyclic Esters. *Macromolecules* **2006**, *39* (25), 8574-8583. DOI: 10.1021/ma0619381.
- (71) Taylor, J. E.; Bull, S. D.; Williams, J. M. Amidines, isothioureas, and guanidines as nucleophilic catalysts. *Chem. Soc. Rev.* **2012**, *41* (6), 2109-2121. DOI: 10.1039/c2cs15288f From NLM Medline.
- (72) Pratt, R. L., BGG; Long, DA; Lundberg, PNP; Dove, AP; Li, H; Wade, CG; Waymouth, RM; Hedrick, JL. Exploration, Optimization, and Application of Supramolecular Thiourea-Amine Catalysts for the Synthesis of Lactide (Co)polymers. *Macromolecules* **2006**, *39* (23), 7863-7871.
- (73) Mu, Q.; Wang, L.; Dunn, C. K.; Kuang, X.; Duan, F.; Zhang, Z.; Qi, H. J.; Wang, T. Digital light processing 3D printing of conductive complex structures. *Addit. Manuf.* **2017**, *18*, 74-83. DOI: 10.1016/j.addma.2017.08.011.
- (74) Podgorski, M.; Becka, E.; Chatani, S.; Claudino, M.; Bowman, C. N. Ester-free Thiol-X Resins: New Materials with Enhanced Mechanical Behavior and Solvent Resistance. *Polym Chem* **2015**, *6* (12), 2234-2240. DOI: 10.1039/C4PY01552E From NLM PubMed-not-MEDLINE.

